Journal of
Mechanics of
Materials and Structures

CONDITIONS FOR THE LOCALISATION OF PLASTIC DEFORMATION IN
TEMPERATURE SENSITIVE VISCOPLASTIC MATERIALS

Martin K. Paesold, Andrew P. Bassom, Klaus Regenauer-Lieb and Manolis Veveakis

∎msp

CONDITIONS FOR THE LOCALISATION OF PLASTIC DEFORMATION IN TEMPERATURE SENSITIVE VISCOPLASTIC MATERIALS

MARTIN K. PAESOLD, ANDREW P. BASSOM, KLAUS REGENAUER-LIEB AND MANOLIS VEVEAKIS

We study the onset of localisation of plastic deformation for a class of materials that exhibit both temperature and rate sensitivity. The onset of localisation is determined via an energy bifurcation criterion, defined by the postulate that viscoplastic materials admit a critical (mechanical) energy input above which deformation becomes unstable and plastic localisation ensues. In analogy to the classical concepts of mechanics, the conditions for the onset of localisation in temperature-sensitive viscoplastic materials are reached at a critical stress. However, it is shown that in viscoplastic materials a material bifurcation occurs when the heat supply through mechanical work surpasses the diffusion capabilities of the material. This transition from near-isothermal stable evolution to near-adiabatic thermal runaway is the well-known concept of shear heating. Here, it is generalised and the correspondence between this runaway instability and the localisation of plastic deformation in solid mechanics is detailed. The obtained phase space controlling the localisation is shown to govern the evolution of the system in the postyield regime. These results suggest that the energy balance essentially drives the evolution of the plastic deformation and therefore constitutes a physics-based hardening law for thermoviscoplastic materials.

1. Introduction

In this work, we present the hypothesis that the classical criterion for localisation can be generalised from their isothermal and adiabatic limits through an extension of an energy bifurcation criterion suggested in earlier studies [Cherukuri and Shawki 1995a; 1995b]. The criterion involves an analytical analysis of the multiple steady states followed by a numerical analysis of the transients. We showcase the development of the criterion, highlight its relation to the characteristics of hyperbolic differential equations (slip line fields) and present a first numerical example. The problem of the localisation of plastic deformation is commonly considered solved once both the spatial configuration of localisation and the necessary loading conditions for its onset are extracted. The classical theory [Hill 1950; 1962; Rudnicki and Rice 1975; Rice 1977] of rate and temperature independent materials, provides a platform upon which modern solid mechanics is built. These works suggest that the spatial configuration as well as the critical loading conditions for the onset of localisation can be obtained from the stationary limit of a material dependent wave equation.

In particular, the slip line field theory for ideal rigid plastic materials has been developed in the middle of the last century [Hill 1950] and successfully applied to metal forming processes. The theory is based on solving the hyperbolic differential equations of mass and momentum balance (at its stationary limit)

and provides a closed form solution for the failure of such an idealised material using the method of characteristics. The slip line field theory [Hill 1962] also forms the background for the development of a criterion of localisation of plastic deformation stemming from a material bifurcation [Rudnicki and Rice 1975; Rice 1977]. The study of this material bifurcation was the subject of the early approaches of accelerating waves in rate and temperature independent solids [Hill 1962; Rudnicki and Rice 1975] and shows that localisation instabilities occur at the stationary wave limit of the linear elasto-plastic wave equation

$$L_{ik}\eta_k = \rho c^2 \eta_i. \tag{1-1}$$

In this eigenvalue problem η_i is the vector of the jump of the velocity gradient, c is the material velocity of the accelerating wave and ρ the material density. The properties of the rate- and temperature-independent material are encapsulated in the acoustic tensor

$$L_{ik} = \nu_j C_{ijkl}^{\text{ep}} \nu_l, \tag{1-2}$$

where C_{ijkl}^{ep} is the elasto-plastic stiffness matrix of the material obeying an incremental elasto-plastic response $\dot{\sigma}_{ij} = C_{ijkl}^{\text{ep}} \dot{\epsilon}_{kl}$. The vectors ν_i are the unit vectors of the discontinuity imposed by the propagating acceleration wave. According to the theory of localisation of plastic deformation [Hill 1962; Rudnicki and Rice 1975], localised failure occurs at the stationary limit of the propagating wave when $c = 0$. In this regime, nontrivial solutions are obtained only when the determinant of the acoustic tensor is zero and this condition allows for the calculation of both the orientation of the localised plane given by the vectors ν_i, and the critical stress ratio for the onset of localisation, given by the critical value of the tangent modulus.

Although slip line field theory has played an undeniable role in underpinning the theory of plasticity, and has still some use in the limit analysis and design [Khan et al. 2008], it has been superseded by advanced numerical techniques that are capable of modelling nonlinear, elastic, viscous and plastic materials [Needleman and Tvergaard 1992]. The main drawback of the slip line field theory was that it cannot be used for rate and temperature dependent constitutive laws which significantly hampered the applicability to modern engineering applications since the importance of temperature is well known in constitutive properties of most materials. Soil, rocks and ceramics are significantly influenced by temperature with strain localisation being strongly affected by thermal loading [Hückel and Baldi 1990; Hückel and Pellegrini 2002]. In polymers and polycarbonates temperature and strain rate are key parameters influencing the response of the material, even at ambient conditions [Bauwens-Crowet et al. 1974]. Finally, even in the analogue rigid materials for which the slip line field theory was developed, i.e., metals, temperature was shown to be important. This becomes obvious in particular under conditions of high speed deformation or at large strain where mechanical work is dissipated and the effects of heat becomes important. An excellent example is the thermal cross that is often observed during forging of mild steel caused by localised plastic dissipation on slip lines [Johnson et al. 1964].

The thermal cross becomes visible as heat lines owing to reaching temperatures of around 680 °C and their pattern [Johnson et al. 1964, Figures 3 and 4]) closely resembles the original slip lines calculated in theoretical plasticity [Hill 1950]. The coincidence of heat lines and slip lines suggests a strong relationship and calls for an extension of the original theory beyond isothermal conditions. Later studies [Benallal and Lemaitre 1991; 2004] generalised the localisation concepts and extended the acoustic tensor

criterion to the realm of coupled thermomechanical response for rate-independent materials, involving an updated formulation of the acoustic tensor for the limits of isothermal and adiabatic conditions.

However, when dealing with rate-dependent thermoplastic coupling, the mathematical study of the eigenvalue problem (1-1) of plasticity breaks down. The procedure for determining the conditions for the onset of localised deformation differs significantly from that of rate-independent materials [Anand et al. 1987]. In this regime, the conditions for the loss of ellipticity that express the material instability leading to localisation is approached through analyses of the full system of field equations, rather than seeking for the loss of ellipticity of the momentum balance. These techniques were first introduced for one-dimensional plastic shear deformation of nonlinear viscous fluids [Gruntfest 1963; Clifton 1980; Bai 1981; 1982]. The one-dimensional problem of simple shear of a temperature dependent viscoplastic layer has also been treated semianalytically [Chen et al. 1989; Leroy and Molinari 1992]. These concepts gave rise to the proposition of an energy based localisation theory in which instabilities emerge when the mechanical input rate rises significantly leading to a departure from the near isothermal limit towards the near adiabatic limit [Cherukuri and Shawki 1995b; 1995a]. Since the energy equation can provide information about the time evolution of the system, this regime has been extensively studied in earth sciences [Regenauer-Lieb et al. 2013a; Regenauer-Lieb et al. 2013b] for one-dimensional failure patterns seen in landslides [Veveakis et al. 2007] and fault mechanics [Veveakis et al. 2010].

The adiabatic limit of the energy equation, also known as adiabatic shear bands, was the focus of considerable research efforts during past decades in material sciences [Gruntfest 1963]. It is of particular interest since the adiabatic shear limit can act as a precursor to failure, irrespective of its mode (ductile or brittle) [Dodd and Bai 2012]. In spite of the apparent relationship suggested by observations such as reported by Johnson et al. [Johnson et al. 1964], a generalised slip line field theory that extends Hill's theory to nonlinear thermoviscoplastic materials is not yet developed. In this study we show that such a theory can be obtained by expanding the conditions necessary for the loss of ellipticity of the momentum equations, in the realm of coupled thermomechanical problems for temperature-dependent, viscoplastic materials. This generalisation of the slip line field theory is two-pronged: firstly, at the limit of stationary thermomechanical wave propagation (following the classical concepts of mechanics) the stress equilibrium conditions define a spatial pattern of failure and dissipation (the product of stress and velocity gradient). Secondly, the energy balance supplies the necessary conditions for the loss of ellipticity that would lead to a jump in the dissipation. Further on, the transient analysis of the system provides the evolution of plastic deformation from near-isothermal to near-adiabatic conditions and verifies the results of the stationary analysis.

In the remainder of this article we present a detailed mathematical approach to the problem. In Section 2 the continuum thermomechanical framework considered in this article is described. Section 3 extends the concepts of the slip line field theory from ideal plastic to viscoplastic materials. This entails a generalisation of Hencky's and Geiringer's equations that determine the geometry and the onset of localisation, respectively. These results are compared to finite element simulations of simple geometries and Johnson's heat lines (see [Johnson et al. 1964, Figures 3 and 4]) in Section 4. We conclude with a discussion on the importance of the obtained results in Section 5. In the appendices more details on the mathematical derivations are given and in Appendix A the energy budget of a viscoplastic material is discussed, Appendix B details the derivation of the slip lines and Appendix C gives a perturbation analysis of the energy equation.

2. Fundamental principles of continuum thermomechanics

Here, we restrict ourselves to general plane strain loading and neglect the effect of gravity and inertia terms so that the stress equilibrium reads

$$\frac{\partial \sigma_{11}}{\partial x_1} + \frac{\partial \sigma_{12}}{\partial x_2} = 0, \tag{2-1}$$

$$\frac{\partial \sigma_{21}}{\partial x_1} + \frac{\partial \sigma_{22}}{\partial x_2} = 0. \tag{2-2}$$

Further, we adopt the stress decomposition $\sigma_{ij} = p\delta_{ij} + s_{ij}$, with p the volumetric mean stress and s_{ij} the deviatoric stress. For such a problem, we formulate the governing equations in the equivalent coordinate system where the stress tensor is rotated such that its elements are the mean stress $p = I_1/3$ and the von Mises stress $q = \sqrt{3J_2}$. In these expressions $I_1 = tr(\sigma_{ij})$ is the first invariant of the stress tensor and $J_2 = s_{ij}s_{ij}/2$. The corresponding coordinate transformation dates back to Levy [Hill 1950] and is given through the Mohr circle transformation

$$\sigma_{11} = p - q\sin 2\psi, \quad \sigma_{22} = p + q\sin 2\psi, \quad \sigma_{12} = \sigma_{21} = q\cos 2\psi, \tag{2-3}$$

where ψ is the rotation angle of the coordinate system.

2A. *Energy considerations.* In this study we neglect higher-order energy terms in the energy equation. These terms are expressed in terms of a second derivative of the Helmholtz free energy, $\frac{\partial^2 \psi}{\partial \psi \partial T}\dot{\xi}$ and are of secondary importance when studying the quasistatic the problem of localisation of viscoplastic deformation. Frequently this is the case because $\dot{\xi} = 0$ at steady state. Such a case is the thermoelastic heating term (see Appendix A) in which case the internal state variable is the elastic strain. Under this assumption, the energy balance combined with the second law of thermodynamics can be written as

$$\rho c \frac{\partial T}{\partial t} = \alpha \left(\frac{\partial^2}{\partial x_1^2} + \frac{\partial^2}{\partial x_2^2} \right) T + \Phi - r_{\text{sink}}, \tag{2-4}$$

where the right hand side represents the temporal change of energy within a volume element due to heat flux and mechanical dissipation

$$\Phi = \beta \sigma_{ij} \dot{\varepsilon}_{ij}^p, \tag{2-5}$$

and an energy sink r_{sink} due to a postlocalisation transformation such as melting or endothermic chemical reactions [Rosakis et al. 2000]. The constants in (2-4)–(2-5) denote the material density ρ, the specific heat capacity c, heat conductivity α and the Taylor–Quinney coefficient β [Taylor and Quinney 1934]. This coefficient quantifies the amount of mechanical work converted to heat and β is of particular importance in the field of thermodynamics with internal state variables, as it incorporates the evolution of all the internal state variables ξ of the system, as evident from its definition [Alevizos et al. 2014; Veveakis et al. 2014]

$$\beta = 1 - \frac{Y\dot{\xi}}{\sigma_{ij}\dot{\varepsilon}_{ij}^p}. \tag{2-6}$$

In this expression Y is a thermodynamic potential, dual in energy with the internal state variable ξ.

2B. *Constitutive modelling.* We first split the strain rate into elastic (reversible) and plastic (irreversible) parts $\dot{\varepsilon}_{ij} = \dot{\varepsilon}_{ij}^e + \dot{\varepsilon}_{ij}^p$. For the elastic component we adopt a linear elastic law of the form

$$\dot{\varepsilon}_{ij}^e = C_{ijkl}^{-1}\dot{\sigma}_{kl}. \tag{2-7}$$

For the irreversible part, we assume that the Helmholtz free energy is invertible, such that the evolution of the plastic strain depends on the stress and temperature through a smooth function of the plastic potential $g(\sigma_{ij}, T)$. We focus on temperature contributions that act independently of the stress such that the viscoplastic flow law can be decomposed as

$$\dot{\varepsilon}_{ij}^p = \dot{\varepsilon}_0\, e^{-T_0/T} \langle f(g) \rangle \frac{\partial g(\sigma_{ij})}{\partial \sigma_{ij}}, \tag{2-8}$$

where the activation temperature is denoted by T_0, and the Macaulay brackets $\langle \cdot \rangle$ ensure zero plastic strain before yield [Freed and Walker 1993]. This decomposition is supported by experimental data at elevated temperatures, below the phase transition temperature of the material [Bauwens-Crowet et al. 1974] and the two most representative constitutive responses of temperature and rate dependent materials are an Arrhenius-type dependency on temperature, with either a power-law or an exponential dependency on stress. The function $f(g)$ is an arbitrary scalar flow stress function. For the example of J_2 associative viscoplasticity the viscoplastic flow law takes the form

$$\dot{\varepsilon}_{ij}^p = \dot{e}_{ij}^p = \dot{\varepsilon}_0\, e^{-T_0/T} \langle f(g) \rangle \frac{\partial g}{\partial s_{ij}} = \dot{\varepsilon}_0 \left\langle \frac{\sqrt{q}}{k} - 1 \right\rangle \frac{s_{ij}}{q}\, e^{-T_0/T}, \tag{2-9}$$

where $\dot{e}_{ij}^p$ is the deviatoric part of the strain-rate plastic and k is the yield stress [Perzyna 1966]. The flow stress function is in principle dependent on temperature, plastic strain and any other internal state variable, but in this study we will not consider these dependencies for simplicity in the mathematical treatment.

The exact form of the constitutive equation is not prescribed during the analysis of the bifurcation in order to emphasise the generic nature of the formulation, where the onset of plastic deformation is derived from the basic assumptions of the energetics. The only important aspect of the constitutive response of the material is that it must obey a viscoplastic relationship linking the plastic strain-rate (i.e., plastic strain increment) with the stress, in contrast to rate independent plasticity where an incremental relationship between plastic strain increment and stress increment is required. The viscoplastic law is required so that in the steady-state limit of the equations ($\dot{\sigma}_{ij} = \dot{T} = 0$) the mechanical dissipation remains nonzero.

The formulation therefore encompasses most classes of physical behaviour described in the summary of constitutive laws for viscoplastic materials [Chaboche 2008]. Since the rate-independent plasticity case can be deduced from the equations of viscoplasticity as a limiting case [Chaboche 1977; Lubliner 2008], the presented formulation can be seen as a generic framework for temperature-sensitive plasticity. For a more detailed discussion on the constitutive concepts of viscoplasticity the reader is encouraged to consult the review article by Chaboche [2008].

As shown in earlier studies [Leroy and Molinari 1992; Cherukuri and Shawki 1995b; Veveakis et al. 2010], the choice of the form of the temperature dependence of the plastic flow law is not central for the results of the present study. Those studies have shown that any nonlinear temperature dependence

leads to the same physical behaviour with the Arrhenius type exponential dependency being the one that allows for the most convenient mathematical treatment.

3. Steady state analysis: generalisation of the slip line field theory

We start by studying the steady-state limit of the system, in which $\dot{T} = \dot{\sigma}_{ij} = 0$. Therefore, in this regime the elastic contribution (2-7) is neglected and the problem reduces to that of the study of the response of a rigid (visco-)plastic material. This setting can therefore be considered to be a direct extension of the slip line field theory to thermoviscoplastic materials. We note that in the present formulation the temperature equation (2-4) is active only when dissipation is nonzero. Since this is achieved in the postyield regime, we expect that the orientation of possible localisation planes would arise from the characteristics of the stress equilibrium, in accordance with the theory of plasticity [Hill 1950].

We therefore anticipate that given an arbitrary set of slip lines, two distinctly different cases of material response can be identified from the energy balance equation. The plastic material may deform homogeneously across the whole domain, and therefore across the slip lines; alternatively the material deforms in a localised manner along the slip lines (the equivalent velocity gradient discontinuities in the classical case). In our formulation the transition becomes an energy based transition expressed through the multiple steady states which are possible. The complete field approach of the present work consists of the identification of the generalised patterns of slip lines given by an arbitrary yield surface and the derivation of the conditions for localised plastic deformation along these slip lines.

3A. *Generalised Hencky's equations.*   At the point of initial yield, where the temperature equation is inactive, the response of the system is governed by the stress equilibrium equations. We assume a generalised yield surface at a reference temperature of the form $q = q_Y(p)$. In order to find the characteristics of the hyperbolic differential stress equilibrium equations (slip lines) we substitute the Levy stress transformations, (2-3), into the stress equilibrium equations, (2-1) and (2-2). The mathematical treatment is detailed in Appendix B (see also [Lubliner 2008, Chapter 5]) and the results are summarised below.

The slip lines are parametrised in terms of the arc-length s and the slopes of the characteristics along the x_1- and x_2-axes read

$$\frac{\partial x_1}{\partial s_k} = \frac{\mu^{(k)}}{\sqrt{1 + \mu^{(k)2}}}, \qquad \frac{\partial x_2}{\partial s_k} = \frac{1}{\sqrt{1 + \mu^{(k)2}}} \qquad (k = 1, 2), \tag{3-1}$$

where $\mu^{(k)}$ is the k-th left eigenvalue of the stress equilibrium equations (see Appendix B). For a general yield surface $q(p)$

$$\mu^{(1,2)} = \frac{\mp\sqrt{1 - h^2} + \cos(2\psi)}{h + \sin(2\psi)}, \tag{3-2}$$

and the quantity $h = q_Y'(p)$ is a generalised pressure modulus. Note that in this expression p must be critical, i.e., equal to its yield value. For incompressible materials $h = 0$.

Rescaling (2-1) and (2-2) along the characteristics, Equation (3-1) provides

$$r_i^{(k)} B_{ij} \frac{\partial(p, \psi)}{\partial s} = 0 \quad (k = 1, 2), \tag{3-3}$$

where the left eigenvectors are

$$r^{(1,2)} = \left(\frac{\sqrt{1-h^2} \mp \cos(2\psi)}{\pm(h - \sin(2\psi))}, \, 1 \right).$$ (3-4)

Equations (3-3) are derived in Appendix B and expanding them yields the generalised Henchky's equations

$$0 = \sqrt{1-h^2} \, p_s \pm 2q\psi_s.$$ (3-5)

In the case of a von Mises material, where $q_Y = k$ is a constant, (3-2) simplifies (as $h = 0$) to the familiar form

$$\mu^{(1)} = -\tan\psi, \quad \mu^{(2)} = \cot\psi,$$ (3-6)

and the eigenvectors (3-4) to

$$r^{(1)} = (-\tan\psi, 1), \quad r^{(2)} = (\cot\psi, 1).$$ (3-7)

The corresponding traces are commonly known as α/β-slip lines. Along the slip lines Equations (3-5) reduce to the classical Hencky's equations

$$p \pm 2k\psi = C_{\alpha,\beta}.$$ (3-8)

3B. *Generalised Geiringer's equations.* Traditionally the velocity components along the slip lines are described by Geiringer's equations which are obtained from the continuity equation, in conjunction with the plastic flow rule and the small-strain compatibility equations [Hill 1950]. In the classical isothermal formulation of slip line field theory velocity solutions are sought that satisfy the continuity equation and localisation of plastic deformation is defined as a velocity jump across the slip line (velocity discontinuity) of zero thickness. In the present formulation we relax the isothermal assumption and seek conditions of localisation that replace the vanishing thickness by a finite width.

To this end, the mechanical dissipation Φ of (2-5) is combined together with the constitutive law of plasticity (2-8) to provide a temperature sensitive dissipation term

$$\Phi = \beta\sigma_{ij}\dot{\varepsilon}_{ij}^p = \beta\dot{\varepsilon}_0\sigma_{ij}\langle f(g)\rangle e^{-T_0/T} \frac{\partial g}{\partial\sigma_{ij}},$$ (3-9)

where the term $\sigma_{ij}(\partial g/\partial\sigma_{ij})$ represents a tensorial product. The stability and bifurcation of the energy balance equation (2-4) is characterised by the nonlinear response of its steady state. This problem has been extensively studied in the literature for shear zones [Gruntfest 1963; Chen et al. 1989; Leroy and Molinari 1992; Vardoulakis 2002; Veveakis et al. 2010]. In this work we generalise it for 2D loading conditions by first studying the response of the energy balance in the original geometry and then rescaling it to a one-dimensional subspace defined by the directions of the characteristics.

3B.1. *Steady state analysis in the original geometry.* The steady state of the energy balance equation is defined by

$$\alpha\left(\frac{\partial^2}{\partial x_1^2} + \frac{\partial^2}{\partial x_2^2}\right) T + \beta\dot{\varepsilon}_0\sigma_{ij}\langle f(g)\rangle \frac{\partial g}{\partial\sigma_{ij}} e^{-T_0/T} = 0.$$ (3-10)

The energy balance can be brought into dimensionless form by setting

$$\theta = \frac{T - T_b}{T_b}, \qquad \hat{x}_i = \frac{x_i}{L_i} \quad (i = 1, 2), \qquad \mathrm{Ar} = \frac{T_0}{T_b}, \tag{3-11}$$

where T_b is the boundary temperature and L_i is an appropriate length scale. Since we are interested in deformation taking place under isothermal boundary conditions the final dimensionless equation is (the superimposed hats are dropped for convenience)

$$\left(\frac{\partial^2}{\partial x_1^2} + \lambda^2 \frac{\partial^2}{\partial x_2^2} \right) \theta + \mathrm{Gr}^{2D} \exp\left(\frac{\mathrm{Ar}\, \theta}{1 + \theta} \right) = 0, \tag{3-12}$$

where $\lambda = L_1 / L_2$ is an aspect ratio and the superscript 2D refers to the dimension of the domain. The exponential term stems from the mechanical dissipation Φ and we define the normalised dissipation function

$$\phi = \exp\left(\frac{\mathrm{Ar}\, \theta}{1 + \theta} \right). \tag{3-13}$$

In order to solve the partial differential equation (3-12) on the domain $[-1, 1] \times [-1, 1]$ a pseudo arc-length continuation [Chan and Keller 1982] in Gr^{2D}, the Gruntfest number [Gruntfest 1963], was carried out where

$$\mathrm{Gr}^{2D} = \frac{\beta \dot{\varepsilon}_0 L_1^2}{\alpha T_b} \sigma_{ij} \langle f(g) \rangle e^{-\mathrm{Ar}} \frac{\partial g}{\partial \sigma_{ij}}, \tag{3-14}$$

and (3-12) is subjected to isothermal boundary conditions

$$\theta(\pm 1, y) = 0, \quad \theta(x, \pm 1) = 0. \tag{3-15}$$

In physical terms, Gr represents the ratio between heat production due to mechanical deformation and heat loss due to thermal conduction or additional energy sinks [Vardoulakis 2002; Veveakis et al. 2010]. At the low Gr limit the system deforms in virtually isothermal conditions, whereas as $\mathrm{Gr} \to \infty$ so the system deforms under near-adiabatic conditions [Veveakis et al. 2010].

It is well known that the steady state response of the system depends on the values of Gr and Ar [Law 2006; Veveakis et al. 2010], see Figure 1. In Figure 1(a) we sketch the maximum temperature at the centre of the domain, θ_c, as a function of Gr for two values of Ar. We notice that between $\mathrm{Ar} = 4$ and $\mathrm{Ar} = 5$ the response of the system changes from a stretched ($\mathrm{Ar} = 4$) to a folded S-curve ($\mathrm{Ar} = 5$). The stability of the system is determined by the eigenvalues of the Jacobian matrix, shown in Figure 1(b). Since the maximum eigenvalue of the case $\mathrm{Ar} \leq 4$ (stretched) is negative for all values of Gr, the stretched S-curve is stable throughout. In contrast, the folded S-curve ($\mathrm{Ar} = 5$) exhibits two points of stability change, coinciding with the turning points of the S-curve. This means that the stationary solutions are initially stable up to the first turning point, then unstable and after the second turning point restabilise.

The above arguments are independent of λ and the variation of the steady state response with respect to λ are presented in Figure 2. This conclusion allows us to proceed with rescaling the energy equation in a 1D equivalent, along the characteristic curves s_k of the stress equilibrium equations.
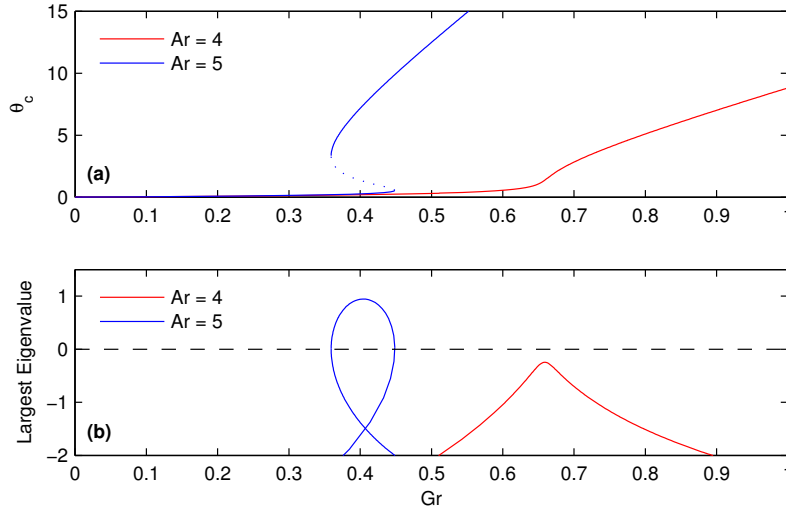
Figure 1. (a) Bifurcation diagram of the two-dimensional heat equation for Ar = 4, 5. If the path of stationary states is folded (Ar = 5) the solutions change stability at the fold and dotted lines denote unstable stationary states. (b) Largest eigenvalues of the Jacobian matrix associated with (3-12). For Ar = 4 the largest eigenvalue remains negative, but for Ar = 5 stability of the stationary solutions changes at the folds where the largest eigenvalue changes sign.
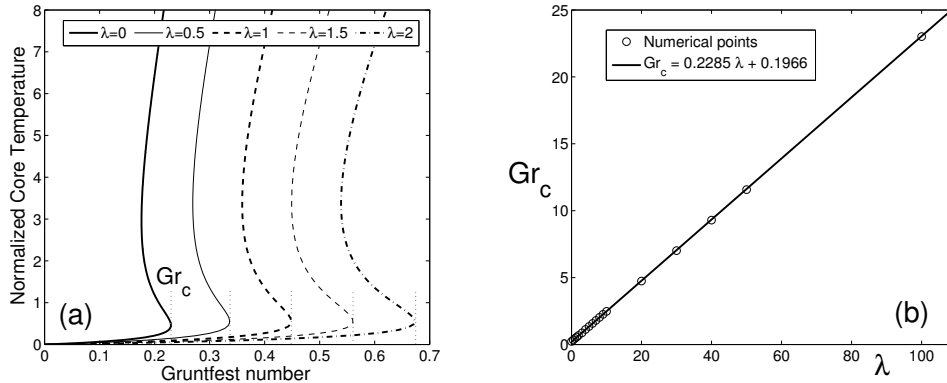

Figure 2. A change in aspect ratio λ shifts the steady states along the Gr-axis, but has only little influence on the shape of the S-curve and no influence on the stability of the steady states.

3B.2. *Rescaling along the characteristics.* In this work we look for the necessary conditions for localisation of the plastic deformation to occur along the characteristics of the stress equilibrium. This means that the characteristic curves s_k also need to be the characteristics of the temperature equation. This condition is satisfied in the limit where the elliptic operator vanishes, which is also the adiabatic limit.

Hence, the loss of ellipticity of the temperature equation would ensure that localisation is achieved along the characteristics of the momentum equation. Localisation should therefore be obtained through the properties of the nonlinear response of the energy equation.

Replacing the spatial derivatives in (3-10) with (3-1) yields

$$\alpha \frac{(1+\mu^2)}{\mu^2}\left((1+\mu^2)\frac{\partial^2}{\partial s^2} + \frac{(\mu^2-1)}{\mu}\frac{\partial \mu}{\partial s}\frac{\partial}{\partial s}\right)T + \beta\dot{\varepsilon}_0 \sigma_{ij}\langle f(g)\rangle\frac{\partial g}{\partial \sigma_{ij}}\,e^{-T_0/T} = 0, \qquad (3\text{-}16)$$

and all super- and subscripts k have been dropped since the above arguments hold true for both sets of characteristics. We consider the case of infinitesimal variations of the slip line geometry, so that the derivatives $\partial\mu/\partial s$ are small and can be ignored.

Analogously to (3-11), (3-16) is normalised and

$$\frac{\partial^2 \theta}{\partial s^2} + \text{Gr}^{1\text{D}}\exp\left(\frac{\text{Ar}\,\theta}{1+\theta}\right) = 0, \qquad (3\text{-}17)$$

where the Gruntfest number admits the following form

$$\text{Gr}^{1\text{D}} = \frac{\beta\dot{\varepsilon}_0 L^2}{\alpha T_b}\frac{\mu^2}{(1+\mu^2)^2}\,e^{-\text{Ar}}\sigma_{ij}\langle f(g)\rangle\frac{\partial g}{\partial \sigma_{ij}}, \qquad (3\text{-}18)$$

where L is a length scale. This Gruntfest number is spatially dependent through μ, and also incorporates the dimensionality of the system at hand, through L and we conjecture that the critical values of the Gruntfest number for the two dimensional and one dimensional case are related via

$$\text{Gr}^{1\text{D}}_{\text{cr}} = \frac{L^2}{L_1^2}\frac{\mu^2}{(1+\mu^2)^2}\,\text{Gr}^{2\text{D}}_{\text{cr}}, \qquad (3\text{-}19)$$

which follows upon comparing (3-14) and (3-18). As an example, we consider the experiment in [Johnson et al. 1964] where the heat lines are oriented along the diagonals of a square sample. When rescaling a von Mises material along the characteristics of a square domain (see the next section) with dimension L_1, then $L = \sqrt{2}L_1$ and the geometric correction

$$\frac{L^2}{L_1^2}\frac{\mu^2}{(1+\mu^2)^2} = \frac{1}{2}$$

as $\mu = -\tan\psi$ or $\mu = \cot\psi$. From here on forward we do not distinct between the $\text{Gr}^{1\text{D}}$ and $\text{Gr}^{2\text{D}}$ any longer since there is no dis-ambiguity in terms of the physics between the one- and two-dimensional heat equation.

The steady state response of this 1D equivalent equation follows that of the 2D case, as shown in Appendix C. In Figure 3, we present the results of this analysis for the dissipation function ϕ and we find three distinct steady states of alternating stability. The unstable branch BC corresponds to a localisation instability across the characteristic trace for the normalised dissipation function ϕ. Since in Figure 3(a) the branches AB and CD are stable in the dissipation the unstable branch BC cannot be admitted and the solution jumps from stable near isothermal homogeneous plastic deformation on AB to localised near adiabatic deformation on CD. The saddle point B therefore corresponds to the necessary condition for the loss of ellipticity of the thermomechanical system, after which localisation is progressively achieved.
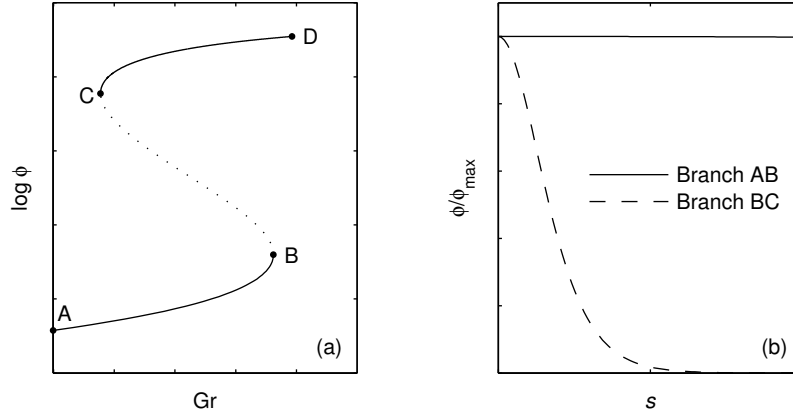
Figure 3. (a) Folded S-curve. Along the branch AB the solution of (3-12) corresponds to an isothermal temperature profile whereas along the section between the turning points B and C the solutions localise. (b) Examples of the one-dimensional spatial pattern of the dissipation profile for Ar = 10. The profiles are normalised with respect to the maximum value of dissipation.

It is a similar condition to the traditional jump conditions for stress and velocity discontinuities in the classical slip line field solution but is expressed here in terms of their product, the dissipation.

This transition from homogeneous to localised deformation is shown in Figure 3(b), where the normalised dissipation is shown to localise towards the centre of the domain as it crosses the unstable BC branch of the S-curve (see also the results of [Leroy and Molinari 1992; Veveakis et al. 2010]). The critical threshold for the transition from the stable branch AB to the new steady state CD is characterised by the turning point B and can be calculated asymptotically as shown in the Appendix C and Figure 10.

4. Transient analysis of the system

The steady state limit characterises the long-term behaviour of the system, but the evolution of the system given a certain initial condition can only be obtained through direct time integration of the transient system of equations of a von Mises elasto-(visco-)plastic material:

$$\frac{\partial \sigma_{ij}}{\partial x_i} = 0, \quad \rho c \frac{\partial T}{\partial t} = \alpha \frac{\partial^2 T}{\partial x_i^2} + \beta s_{ij} \dot{e}_{ij}^p, \quad \dot{e}_{ij} = \frac{\dot{s_{ij}}}{2G} + \dot{\varepsilon}_0 \left\langle \frac{\sqrt{q}}{k} - 1 \right\rangle \frac{s_{ij}}{q} e^{-T_0/T}. \tag{4-1}$$

where G is the elastic shear modulus, and the last term of the third equation corresponds to the viscoplastic contribution of an associative von Mises material. Notably, although the momentum balance is at its stationary limit, the time evolution of the system is achieved through the temperature equation. The energy balance therefore acts as a postfailure evolution equation similar to the ad hoc evolution laws of the hardening modulus in classical plasticity.

In this section, we integrate this system of equations for the case of an ideal viscoplastic ($G \to \infty$) and an elasto-viscoplastic material with thermomechanical coupling. To illustrate the results of the steady-state analysis an elementary problem set is chosen, where in a plane strain setting the loading conditions shown in Figure 4 are applied. A square cell is pinned in the x, y-direction on the left hand side and in
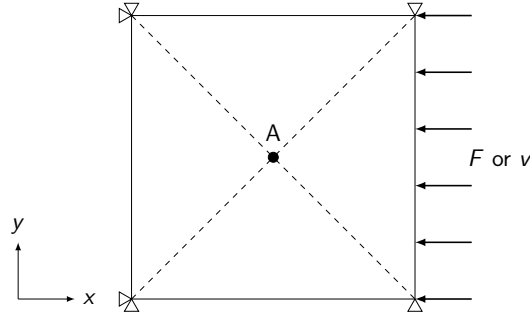
Figure 4. Geometry of the problem configuration. A square is deformed by applying either a constant force F or constant velocity v at the right hand side of the sample. The sample is pinned on the left and in the y-direction. At the centre "A" the sample is probed for various quantities. The theoretical analysis presented in the previous sections for a rate-dependent von Mises material suggests that the slip lines of this model run diagonally across the specimen and are represented by dashed lines [Johnson et al. 1964].

the y-direction on the right hand side. It is loaded on the right boundary with either a constant force F or constant velocity v. The cell is surrounded by a reservoir that has a constant temperature T_b.

The results of the previous sections suggest that in such a configuration the slip lines should propagate from the pinned corners of the rectangle, diagonally across the specimen as discussed in [Johnson et al. 1964]. Owing to the pressure independent von Mises yield envelope, the slip lines are expected to be perpendicular to each other. In addition, the critical condition for the localisation of plastic deformation is expected to be given by the critical value of the Gruntfest number, as shown in the previous sections. In the time-dependent case, we may follow the same rules of normalisation ((3-11)) and define the Gruntfest number as

$$\mathrm{Gr} = \left(\frac{\beta \dot{\varepsilon}_0 L^2}{4\alpha T_b} e^{-\mathrm{Ar}} \right) s_{ij} \left\langle \frac{q}{k} - 1 \right\rangle. \tag{4-2}$$

Because the Gruntfest number incorporates the mechanical work, we expect the Gruntfest analysis of the previous section to hold for both constant force and constant velocity conditions. The difference between the two regimes would be that in the case of constant force conditions Gr will obtain a constant value, once the stress equilibrates to a constant value. Under constant velocity conditions, the stress, and so Gr, will continue to increase throughout the time of loading. Therefore, given enough time the system will always be able to cross the critical Gr value for the onset of localisation.

In the following sections we present the results of the time-integration of the system (4-1). The analysis was carried out using finite element techniques as implemented in the finite element code REDBACK[1] in which the viscoplasticity is solved using Perzyna's overstress formulation. REDBACK is an open source application derived from the *Multiphysics Object Oriented Simulation Environment* (MOOSE) [Gaston et al. 2009]. MOOSE provides a simulation environment that is focussed on the physics of the problem at hand and it takes care of meshing and numerical handling of memory and structures internally via the finite element library libMesh [Kirk et al. 2006] and the nonlinear parallel solver PETSc

[1]Available at http://github.com/pou036/redback.git.

[Balay et al. 2014], respectively. Hence, MOOSE's approach to the finite element method is mesh and dimension independent which differentiates it from other solvers that require the user to define elements and handle more in-depth numerical issues. MOOSE is based in Jacobian-free Newton–Krylov methods for computational efficiency [Knoll and Keyes 2004].

Initially we present two cases for the deformation of an ideal viscoplastic material and an elasto-viscoplastic material under constant force boundary conditions. Further, the response of the elasto-viscoplastic material under a constant velocity boundary condition is studied.

4A. *Ideal viscoplastic material under constant force boundary conditions.* In the case of an ideal viscoplastic material ($G \to \infty$) under constant force conditions the stress exerted onto the sample is constant throughout the simulation and the sample enters the plastic regime immediately. Hence, Gr is held constant throughout the loading. The evolution of the deforming system is best represented by its orbits in Gr-θ space as shown in Figure 5 because this allows for a direct comparison between the "S-curve" that marks the steady states in Gr-T space and the steady state attained by the sample. As Gr is constant these orbits are vertical lines in the case of ideal viscoplasticity. Figure 5 summarises the evolution of the deforming sample for various initial conditions (marked by grey squares) and their final state (black squares). The results of these simulations confirm the concept of the "S-curve" that is comprised of two stable branches that are linked by an unstable branch (BC). If Gr is chosen to be larger than the critical value (turning point B) or the initial state lies above the unstable branch BC the system converges to the high-energy (temperature), adiabatic branch. On the other hand, if Gr is smaller than the critical value the system converges to the low-energy (temperature) isothermal branch.

When elasticity is incorporated and the system is loaded using constant force, the Gruntfest number (i.e., the overstress) is expected to relax to a constant value after its initial evolution due to the elastic
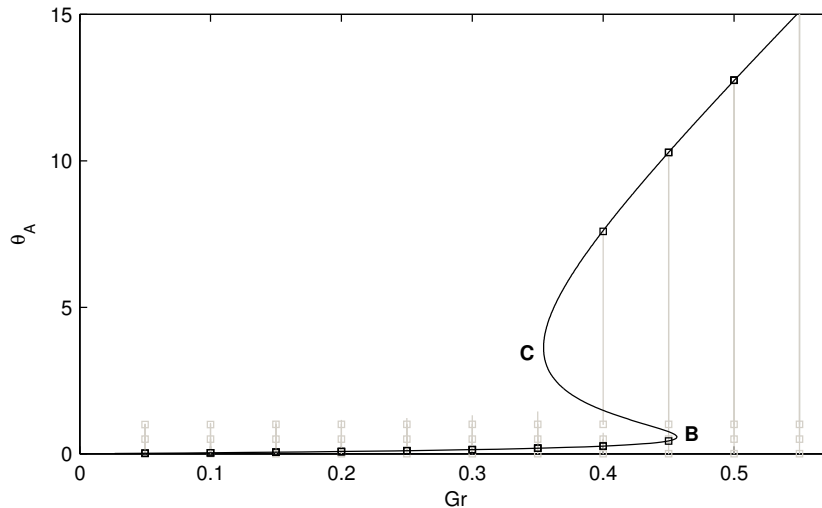

Figure 5. Evolution of an ideal viscoplastic material that is deformed with a constant force. The solid black line marks steady states. The grey lines represent the trajectories through the Gr-θ space as the system evolves in time. Initial and final conditions are marked by grey and black squares, respectively.

response of the system. This regime allows us to test the extent of the validity of the S-curve concept established in Section 3B, since the orbits of the elasto-viscoplastic material are not constant in Gr. To this end, the system of equations (4-1) was integrated for different initial conditions and values of Gr. The results are summarised in Figure 6(a) where we observe that the phase space is indeed split into two domains, in accordance with the concept of the S-curve. Grey squares denote initial conditions and black squares denote the final state of each numerical experiment.

For initial conditions starting below the unstable branch (branch BC of Figure 3) the system evolves towards a low-energy steady state, which coincides with the stable branch AB of Figure 3. Correspondingly, for initial conditions above the unstable branch the orbits diverge and eventually relax in a high-energy steady-state where dissipation localises along the characteristics of the stress equilibrium equations. This high energy steady state corresponds to the branch CD of Figure 3. Runs that started very close to, but above, branch BC (solid black squares) diverge towards the high temperature branch as well. The time evolution of these orbits showcase the different responses (Figure 6(b,c)). Indeed, the low-energy orbits converge quickly to the low-energy steady state where plastic deformation is not localised, whereas the high-energy orbits provide an evolution of the system towards the localisation of dissipation along the characteristics of the stress equilibrium equations. This transition is equivalent to the evolution from secondary to tertiary creep in material science (Figure 6(b,c)).

4B. *Elasto-viscoplastic material under constant force boundary conditions.* Following the results of Figure 3, we expect the orbits leading to the low-energy steady state to be stable without profound localisation of the plastic deformation. On the contrary, the high-energy steady-state is expected to provide the necessary conditions for localisation. In Figure 7 we plot the spatial distribution of the mechanical dissipation for an orbit converging to a low-energy and high-energy steady-state. We notice that in both cases the slip lines indeed propagate from the corners towards the diagonals of the specimen as expected, but that in the low-energy case the plastic deformation is not localised across the slip lines, whereas in the high energy case localisation is emerging, with localisation being more pronounced the higher the value of Gr. We may therefore suggest indeed that the critical Gruntfest number constitutes a material bifurcation criterion for temperature sensitive viscoplastic materials.

4C. *Heat lines under constant velocity boundary conditions.* When the elasto-viscoplastic material is loaded at constant velocity conditions, the Gruntfest number initially grows rapidly and attains values beyond its critical value. Hence, the temperature rises rapidly and the system can be assumed to transition quickly from near-isothermal to near-adiabatic conditions.

An extreme end-member of this regime is the case of an elasto-viscoplastic material evolving under fast loading, thus establishing directly adiabatic conditions. This regime which is also known as adiabatic shear banding is crucial in metal forming and cutting [Gruntfest 1963], but also in geomaterials [Vardoulakis 2002]. In the present study adiabatic shear banding constitutes just a limiting case of the analysis, when Gr → ∞. Such a case can be simulated by setting the thermal diffusion to zero in the temperature equation which is equivalent to assuming that the diffusive capabilities of the material are negligible as compared to the heat producing capabilities. In this case, the dimensionless form of the temperature equation (4-1) reads

$$\frac{\partial \theta}{\partial t_{\text{ad}}} = \exp\left(\frac{\theta}{1 + \epsilon\theta}\right), \tag{4-3}$$
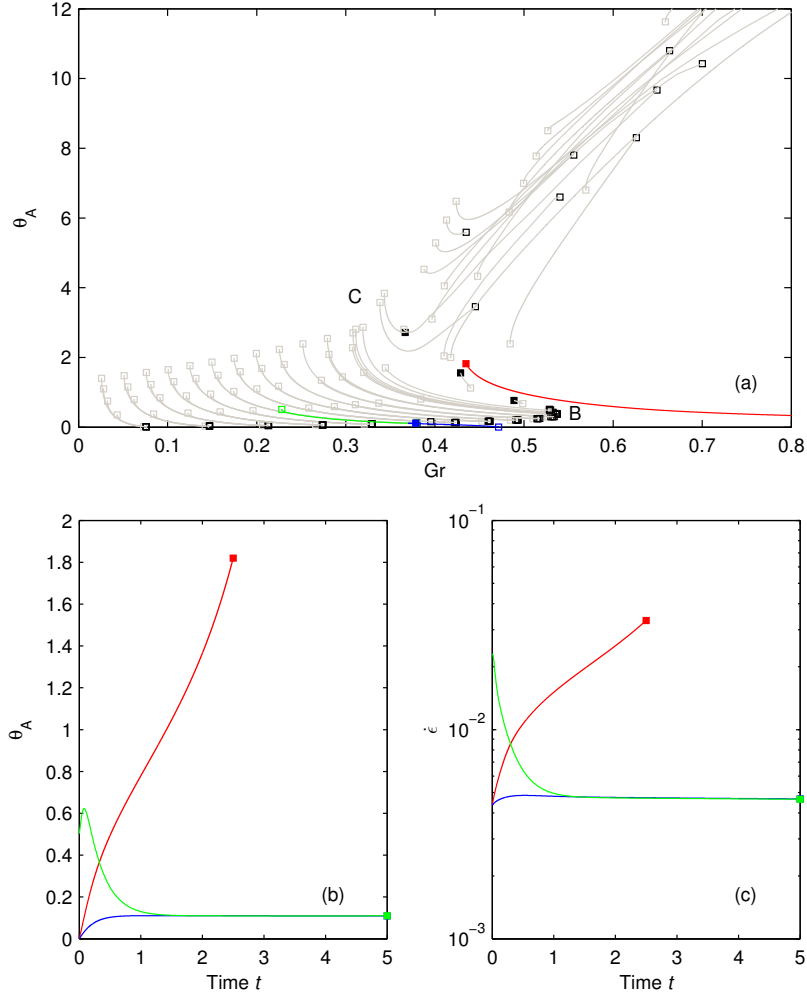
Figure 6. (a) Evolution of an elasto-viscoplastic material deformed with a constant force. Grey and black squares mark initial and final states of the system of the simulation, respectively. The solid black squares mark the final state of runs with initial conditions very close to but above the separatrix BC and we find that the these runs are indeed intrinsically unstable, blowing up in short times. (b) Centre temperature θ_A over time for the three runs marked in (a). (c) Strain rate $\dot{\varepsilon}$ at point A over time for the three runs marked in (a).

where $t_{\mathrm{ad}} = \mathrm{Gr} \cdot t$ is finite only when $t \to 0$, since $\mathrm{Gr} \to \infty$. This means that the limiting case of adiabatic shearing takes place in explosive timescales of the order $t \sim \mathbb{O}(1/\mathrm{Gr})$ [Gruntfest 1963; Veveakis et al. 2007]. Hence, the Gruntfest number Gr controls the time evolution of the adiabatic shear banding, in addition to the onset of localisation.

Under such a scenario the localisation of dissipation along the slip lines is profound, and patterns resembling the heat lines of [Johnson et al. 1964] are obtained, as shown in Figure 8. In this case the system enters directly the unstable area of the S-curve, and traces the upper branch CD during the time of loading.
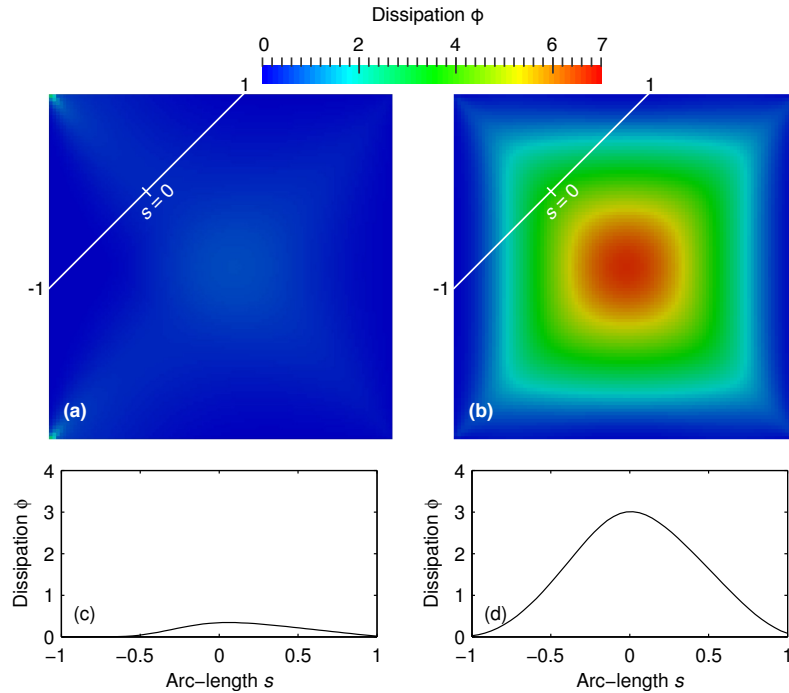
Figure 7. Dissipation profiles for the final state of a run that converges towards the low temperature branch AB and a run that converges towards branch CD. The spatial distribution of the mechanical dissipation: (a) isothermal low temperature stable branch without significant localisation of plastic deformation. (b) simulation for the high temperature branch with significant localised heating. The dissipation profiles were recorded along the lines highlighted in (a) and (b) and are presented in (c) and (d), respectively.
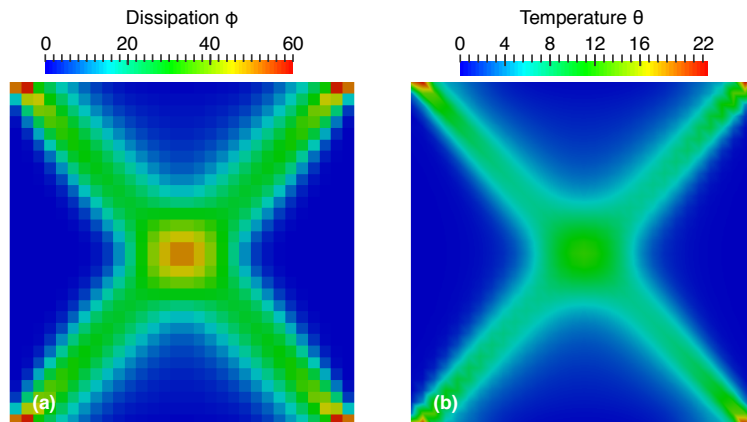
Figure 8. Heat lines under fast constant velocity loading. The heat lines emerge from an initially homogeneous temperature state. The heat lines follow the slip lines and can be observed as a localisation of (a) mechanical dissipation and (b) temperature.

5. Discussion

The simulation of the temporal evolution of temperature and rate-sensitive materials under various loading conditions verifies the results of the steady-state response. In conclusion, the problem of mechanical deformation of a temperature-sensitive viscoplastic material can be elegantly captured by the bifurcation curves of Figure 1. We have seen that for this class of materials the energy equation determines the conditions for the onset of localisation of plastic deformation, which occurs along the characteristics of the stress equilibrium equations.

The results of Figure 6 highlight this energy bifurcation as the main driver of the transient orbits in the system, even when elasticity is considered. It therefore provides a material bifurcation criterion and, combined with the analysis of Section 3A, a generalisation of the slip line field theory for thermoviscoplastic materials. The main effect of an extension to rate and temperature dependence is that lines of velocity discontinuity do not exist below a critical temperature and deformation rate corresponding to a critical dissipation as captured by the Gruntfest number Gr. Above critical Gr the classical slip lines emerge in terms of velocity discontinuities and below critical Gr homogeneous deformation is derived.

The extension of the analytical treatment of generalised slip line field theory to the transient regime using a numerical scheme has allowed us to test it for the problem of metal forging [Johnson et al. 1964]. The constant velocity boundary condition applied during forging lead to a variation in Gr thereby crossing the stability regimes from homogeneous deformation to the appearance of heat lines. The fast loading during this deformation can lead the material directly to the extreme case of adiabatic deformation.

This work has therefore presented a generalised approach of slip line field theory showing that the simple, but restrictive, rheology of a rigid-plastic body can be extended to included rate dependent and temperature dependent material behaviour. We have detailed an energy based framework to obtain the modified Hencky's and Geiringer's equations which still provide the information on the basic pattern of slip lines underpinning the deformation process. We argue that this extension is therefore useful for gaining a basic understanding into the more complex material behaviour from an analytical perspective. The extension of the analytical approach reveals, however, a more complex material behaviour than in the classical theory.

The results of the present study highlight the role of the energy balance in material bifurcations. Since the critical condition for material instability is retrieved from an energy bifurcation, the temperature equation can act as a hardening law and substitute the experimentally derived hardening laws. Such a case would allow us to account explicitly for different physics as well as for the mechanisms acting at different scales in a material through their energy budget. We are therefore one step further to our quest on multiscale analyses, since all the necessary mechanisms can be explicitly accounted for in the energy equation through the corresponding internal state variables of the microprocesses. The results of the present work can provide the basis for a unified theory for material behaviour, starting from solid mechanics and extending naturally to the fluid-like postfailure evolution of materials using explicitly the energy considerations as the link.

Appendix A: The complete energy budget

A consistent description of the thermomechanical behaviour of viscoplastic materials must be based on the conservation of (1) mass, (2) momentum and (3) energy. In addition to these conservation laws

it must be ensured that the entropy production is positive at all times. The combination of these four prerequisites leads to the heat equation

$$\rho c \dot{T} = \partial_{x_i} \alpha \partial_{x_i} T + \Phi + r + T(\partial_T \sigma_{ij}) \dot{\varepsilon}_{ij}^e \tag{A-1}$$

that describes the local energy budget and where ρ denotes the material density, c the specific heat, α the heat conductivity, Φ the mechanical dissipation, σ_{ij} the stress tensor, $\dot{\varepsilon}_{ij}^e$ the elastic strain rate. The significance of this equation is that it couples the temperature evolution to the mechanical properties of the material.

In the context of thermomechanical coupling the term r in (A-1) could be thought of as a heat sink that has the effect of limiting temperature production after the onset of localisation. Possible heat sinks due to a postlocalisation transformation are melting or endothermic chemical reactions [Rosakis et al. 2000]. Without the heat sink uncontrolled thermal runaway would ensue and hence r acts as a stabiliser [Veveakis et al. 2010]. In this work r is neglected, because the aim of this work is to find criteria for the onset of localisation and a detailed study of the postlocalisation regime is not of central interest. In doing so, the postfailure evolution of temperature will be exaggerated, since the heat-absorbing processes gathered in r do not limit the temperature evolution.

The final term in (A-1) describes thermoelastic heating, but is ignored in this work for simplicity of the mathematical treatment.

Appendix B: Characteristic traces and generalised Hencky equations

Here, the stress equilibrium equations (2-1) and (2-2) are rewritten as a system of first-order differential equations by means of the method of characteristics and this process reveals the characteristic traces inherent to the stress equilibrium equations. In the context of plasticity characteristic traces are often referred to as slip lines along which failure will occur [Hill 1950]. Hence, in the remainder of this section the geometry of the failure patterns is determined.

Rather than solving equations (2-1) and (2-2) for the stress components σ_{ij} themselves we employ the Mohr circle transformation (2-3) and evaluate p, q and ϕ. Since there are three unknowns and only two equations a further relation is required and we choose a general yield criterion that allows to express q in terms of p, $q = q(p)$.

After substituting the stress components (2-3), (2-1) and (2-2) can be conveniently written in matrix form as

$$A_{ij} \frac{\partial(p, \psi)}{\partial x_1} + B_{ij} \frac{\partial(p, \psi)}{\partial x_2} = 0, \tag{B-1}$$

where

$$A = \begin{pmatrix} 1 - q' \sin(2\psi) & -2q \cos(2\psi) \\ q' \cos(2\psi) & -2q \sin(2\psi) \end{pmatrix}, \tag{B-2}$$

$$B = \begin{pmatrix} q' \cos(2\psi) & -2q \sin(2\psi) \\ q' \sin(2\psi) + 1 & 2q \cos(2\psi) \end{pmatrix}, \tag{B-3}$$

and the prime $(\cdot)'$ denotes differentiation with respect to p. In order to simplify (B-1) the two (left) eigenvectors r_i and eigenvalues μ that satisfy

$$r_i^{(k)} A_{ij} = \mu^{(k)} r_i^{(k)} B_{ij} \quad (k = 1, 2) \tag{B-4}$$

are computed and (B-4) is substituted into (B-1) so that

$$r_i^{(k)} B_{ij} \left(\frac{\mu^{(k)}}{\sqrt{1 + \mu^{(k)2}}} \frac{\partial(p, \psi)}{\partial x_1} + \frac{1}{\sqrt{1 + \mu^{(k)2}}} \frac{\partial(p, \psi)}{\partial x_2} \right) = 0. \tag{B-5}$$

Instead of solving (B-5) on the whole x_1-x_2 plane we restrict ourselves to one characteristic trace along which the independent variables x_1 and x_2 can be parametrised in terms of the arc-length s. Parametrising along the characteristic and identifying

$$\frac{\partial x_1}{\partial s_k} = \frac{\mu^{(k)}}{\sqrt{1 + \mu^{(k)2}}}, \quad \frac{\partial x_2}{\partial s_k} = \frac{1}{\sqrt{1 + \mu^{(k)2}}} \tag{B-6}$$

allows us to write (B-5) as

$$r_i^{(k)} B_{ij} \frac{\partial(p, \psi)}{\partial s_k} = 0, \tag{B-7}$$

and the coupled system of ordinary differential equations (B-6) and (B-7) is equivalent to stress equilibrium equations (2-1)–(2-2) along the characteristic.

We wish to emphasise that (B-6) defines the geometry of the characteristic trace and that there are two characteristic traces. In general, the eigenvalues $\mu^{(k)}$ depend on ψ and $q'(p)$.

Appendix C: Asymptotic approximations

In this section asymptotic solutions to the nondimensional heat equation (3-12) are computed, but the perturbation analysis requires us to identify a "small" parameter which is used as the perturbation parameter. If the temperature is measured in units of Ar such that $\tilde{\theta} = \mathrm{Ar}\, \theta$ the heat equation (3-16) reads

$$\tilde{\theta}'' + \widetilde{\mathrm{Gr}} \exp\left(\frac{\tilde{\theta}}{1 + \varepsilon \tilde{\theta}} \right), \tag{C-1}$$

where $\widetilde{\mathrm{Gr}} = \mathrm{Ar}\, \mathrm{Gr}$ and $\varepsilon = 1/\mathrm{Ar} \ll 1$ and ε is a suitable perturbation parameter. We drop the $\sim$ superscript for convenience.

If $\theta \sim \mathbb{O}(1)$, $\varepsilon\theta \ll 1$ and the exponent in (C-1) can be expanded as a geometric series which yields

$$\theta'' + \mathrm{Gr} \exp(\theta - \varepsilon\theta^2 + \varepsilon^2\theta^3 + \cdots) = 0. \tag{C-2}$$

In order to find the governing equations at increasing orders of ε we expand

$$\theta = \theta_0 + \varepsilon\theta_1 + \cdots \quad \text{and} \quad \mathrm{Gr} = \mathrm{Gr}_0 + \varepsilon\, \mathrm{Gr}_1 + \cdots$$

and substitute into (C-2). Here, only asymptotic solutions up to $\mathbb{O}(\varepsilon^2)$ are considered and we find

$$0 = (\theta_0 + \varepsilon\theta_1 + \varepsilon^2\theta_2 + \cdots)'' + (\mathrm{Gr}_0 + \varepsilon\, \mathrm{Gr}_1 + \varepsilon^2\, \mathrm{Gr}_2 + \cdots)$$
$$\times \exp(\theta_0 + \varepsilon(\theta_1 - \theta_0^2) + \varepsilon^2(\theta_2 - 2\theta_0\theta_1 + \theta_0^3) + \cdots). \tag{C-3}$$

We perturb Gr as well since the previously obtained numerical results suggest that the critical value of the Gruntfest number, Gr_c, depends on Ar, and hence on the small parameter $\varepsilon = Ar^{-1} \ll 1$ (Figure 10).

After the exponential in the above expression is expanded as a Taylor series the zeroth-, first- and second-order equations of an asymptotic series are obtained:

$$\mathbb{O}(1): \quad \theta_0'' + Gr_0 \, e^{\theta_0} = 0, \tag{C-4}$$

$$\mathbb{O}(\varepsilon): \quad \theta_1'' + Gr_0 \, e^{\theta_0}\theta_1 = Gr_0 \, \theta_0^2 e^{\theta_0} - Gr_1 \, e^{\theta_0}, \tag{C-5}$$

$$\mathbb{O}(\varepsilon^2): \quad \theta_2'' + Gr_0 \, e^{\theta_0}\theta_2 = Gr_0 \, e^{\theta_0}\left(2\theta_0\theta_1 - \theta_0^3 - \tfrac{1}{2}(\theta_1 - \theta_0^2)^2\right) - Gr_1 \, e^{\theta_0}(\theta_1 - \theta_0^2) - Gr_2 \, e^{\theta_0}. \tag{C-6}$$

Equation (C-4) has a known solution

$$\theta_0(s) = \theta_c - 2\ln\cosh\left(\sqrt{\frac{Gr_0}{2}}\,e^{\theta_c/2}s\right), \tag{C-7}$$

which satisfies the boundary conditions $\theta_0(0) = \theta_c$ as $\theta_0'(0) = 0$ [Fowler 1997]. The remaining boundary condition, $\theta_0(1) = 0$ fixes the value of Gr_0 and

$$Gr_0 = 2\,\mathrm{acosh}^2[e^{\theta_c/2}]e^{-\theta_c}. \tag{C-8}$$

Maximising Gr_0 with respect to θ_c yields the critical value of Gr at leading order which is $Gr_{0,cr} \approx 0.878$.

In order to find the first-order approximations we note that the homogeneous part of (C-5) is solved by $t_\alpha = \theta_0'$ and $t_\beta = s\theta_0' + 2$. Based on the homogeneous solutions a particular solution t_p can be constructed and we set $t_p = \xi t_\alpha + \psi t_\beta$. The parameters ξ and ψ are required to satisfy

$$0 = \xi' t_\alpha + \psi' t_\beta, \tag{C-9}$$

$$Gr_0 \, \theta_0^2 e^{\theta_0} - Gr_1 \, e^{\theta_0} = \xi' t_\alpha' + \psi' t_\beta'. \tag{C-10}$$
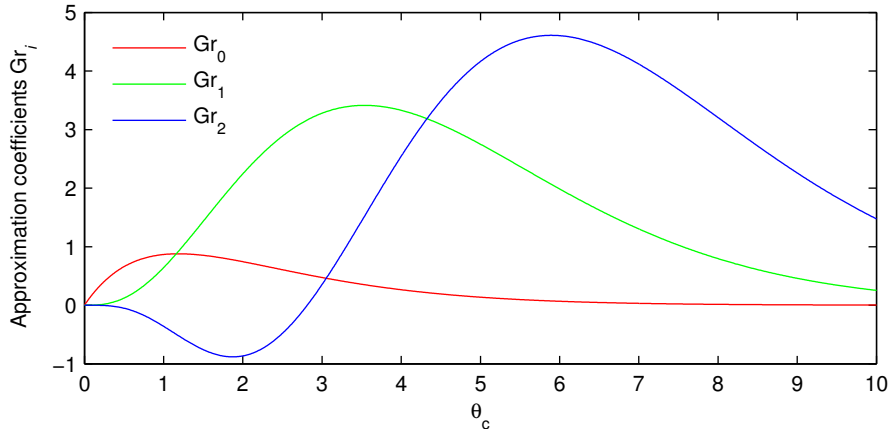
Figure 9. Approximation coefficients Gr_i ($i = 1, 2, 3$) as a function of centre temperature θ_c.
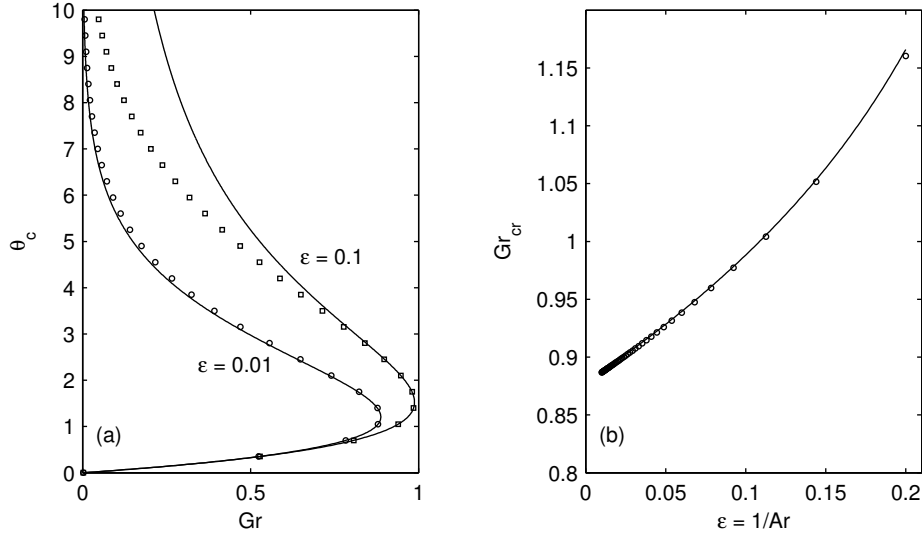
Figure 10. (a) Position of steady states of the heat equation (3-12) for $\varepsilon = 0.1, 0.01$. Squares and circles denote numerical results and the solid lines represent a three-term asymptotic approximation. The asymptotic approximation is suitable for $\theta_c < 3$. (b) The critical Gruntfest number, $\mathrm{Gr_{cr}}$, as a function of ε. Circles denote numerical results and the solid line represents a three-term asymptotic approximation. Note: here temperature is measured in units of Ar as described in the main text.

The even solution of (C-5) then reads

$$\theta_1 = \theta_0^2 - 2\theta_0 + 4s\theta_0' + 6 - \frac{\mathrm{Gr}_1}{\mathrm{Gr}_0} - 2\theta_0' \int \theta_0 \, ds + C_1(s\theta_0' + 2), \qquad \text{(C-11)}$$

where Gr_1 and C_1 are fixed by the boundary conditions $\theta_1(0) = \theta_1(1) = 0$. After θ_1 and Gr_1 have been established the second order corrections Gr_2 and θ_2 can be computed analogously to the first-order correction.

In Figure 9 the coefficients of the expansion $\mathrm{Gr} = \mathrm{Gr}_0 + \mathrm{Gr}_1 \, \varepsilon + \mathrm{Gr}_2 \, \varepsilon^2$ are shown as functions of the centre temperature θ_c and Figure 10(a) presents a comparison of the numerical results and asymptotic approximation. An approximation in the low temperature regime is capable of estimating the critical Gruntfest number to a good degree (see Figure 10(b)).

References

[Alevizos et al. 2014] S. Alevizos, T. Poulet, and E. Veveakis, "Thermo-poro-mechanics of chemically active creeping faults, 1: theory and steady state considerations", *J. Geophys. Res.: Solid Earth* **119**:6 (2014), 4558–4582.

[Anand et al. 1987] L. Anand, K. H. Kim, and T. G. Shawki, "Onset of shear localization in viscoplastic solids", *J. Mech. Phys. Solids* **35**:4 (1987), 407–429.

[Bai 1981] Y. L. Bai, "A criterion for thermo-plastic shear instability", pp. 277–284 in *Shock waves and high-strain-rate phenomena in metals*, edited by M. A. Myers and L. E. Murr, Plenum Press, New York, 1981.

[Bai 1982] Y. L. Bai, "Thermo-plastic instability in simple shear", *J. Mech. Phys. Solids* **30**:4 (1982), 195–207.

[Balay et al. 2014] S. Balay, S. Abhyankar, M. F. Adams, J. Brown, P. Brune, K. Buschelman, V. Eijkhout, W. D. Gropp, D. Kaushik, M. G. Knepley, L. C. McInnes, K. Rupp, B. F. Smith, and H. Zhang, "PETSc Users Manual", software manual ANL-95/11, Argonne National Laboratory, 2014, http://www.mcs.anl.gov/petsc.

[Bauwens-Crowet et al. 1974] C. Bauwens-Crowet, J. M. Ots, and J. Bauwens, "The strain-rate and temperature dependence of yield of polycarbonate in tension, tensile creep and impact tests", *J. Mater. Sci.* **9** (1974), 1197–1201.

[Benallal and Bigoni 2004] A. Benallal and D. Bigoni, "Effects of temperature and thermo-mechanical couplings on material instabilities and strain localization of inelastic materials", *J. Mech. Phys. Solids* **52**:3 (2004), 725–753.

[Benallal and Lemaitre 1991] A. Benallal and J. Lemaitre, "Creep in structures", pp. 223–235 in *Creep in structures: Fourth IUTAM Symposium* (Cracow, Poland, 1990), edited by M. Życzkowski, Springer, Berlin, 1991.

[Chaboche 1977] J. L. Chaboche, "Viscoplastic constitutive equations for the description of cyclic and anisotropic behavior of metals", *B. Acad. Pol. Sci. Tech.* **25**:1 (1977), 33–42.

[Chaboche 2008] J. L. Chaboche, "A review of some plasticity and viscoplasticity constitutive theories", *Int. J. Plast.* **24**:10 (2008), 1642–1693.

[Chan and Keller 1982] T. F. C. Chan and H. B. Keller, "Arc-length continuation and multigrid techniques for nonlinear elliptic eigenvalue problems", *SIAM J. Sci. Stat. Comput.* **3**:2 (1982), 173–194.

[Chen et al. 1989] H. T. Chen, A. S. Douglas, and R. Malek-Madani, "An asymptotic stability condition for inhomogeneous simple shear", *Quart. Appl. Math.* **47**:2 (1989), 247–262.

[Cherukuri and Shawki 1995a] H. Cherukuri and T. Shawki, "An energy-based localization theory, II: effects of the diffusion, inertia, and dissipation numbers", *Int. J. Plast.* **11**:1 (1995), 41–64.

[Cherukuri and Shawki 1995b] H. P. Cherukuri and T. G. Shawki, "An energy-based localization theory, I: basic framework", *Int. J. Plast.* **11**:1 (1995), 15–40.

[Clifton 1980] R. J. Clifton, "Material response to ultra high loading rates", Report No. NMAB-356, NRC National Material Advisory Board (US) Report, 1980.

[Dodd and Bai 2012] B. Dodd and Y. Bai (editors), *Adiabatic shear localization: frontiers and advances*, 2nd ed., Elsevier, 2012.

[Fowler 1997] A. C. Fowler, *Mathematical models in the applied sciences*, Cambridge University Press, 1997.

[Freed and Walker 1993] A. D. Freed and K. P. Walker, "Viscoplasticity with creep and plasticity bounds", *Int. J. Plast.* **9**:2 (1993), 213–242.

[Gaston et al. 2009] D. Gaston, C. Newman, G. Hansen, and D. Lebrun-Grandi, "MOOSE: A parallel computational framework for coupled systems of nonlinear equations", *Nucl. Eng. Des.* **239**:10 (2009), 1768–1778.

[Gruntfest 1963] I. Gruntfest, "Thermal feedback in liquid flow: plane shear at constant stress", *Trans. Soc. Rheol.* **7** (1963), 195–207.

[Hill 1950] R. Hill, *The mathematical theory of plasticity*, Clarendon Press, Oxford, 1950.

[Hill 1962] R. Hill, "Acceleration waves in solids", *J. Mech. Phys. Solids* **10** (1962), 1–16.

[Hückel and Baldi 1990] T. Hückel and G. Baldi, "Thermoplastic behavior of saturated clays: an experimental constitutive study", *J. Geotech. Eng.* **116**:12 (1990), 1778–1796.

[Hückel and Pellegrini 2002] T. Hückel and R. Pellegrini, "Reactive plasticity for clays: application to a natural analog of long-term geomechanical effects of nuclear waste disposal", *Eng. Geology* **64** (2002), 195–215.

[Johnson et al. 1964] W. Johnson, G. L. Baraya, and R. A. C. Slater, "On heat lines or lines of thermal discontinuity", *Int. J. Mech. Sci.* **6**:6 (1964), 409–414.

[Khan et al. 2008] I. A. Khan, V. Bhasin, J. Chattopadhyay, and A. K. Ghosh, "On the equivalence of slip-line fields and work principles for rigid-plastic body in plane strain", *Int. J. Solids Struct.* **45**:25-26 (2008), 6416–6435.

[Kirk et al. 2006] B. S. Kirk, J. W. Peterson, R. H. Stogner, and G. F. Carey, `libMesh`: A C++ library for parallel adaptive mesh refinement/coarsening simulations", *Eng. Comput.* **22**:3-4 (2006), 237–254.

[Knoll and Keyes 2004] D. A. Knoll and D. E. Keyes, "Jacobian-free Newton–Krylov methods: a survey of approaches and applications", *J. Comput. Phys.* **193**:2 (2004), 357–397.

[Law 2006] C. Law, *Combustion physics*, Cambridge University Press, 2006.

[Leroy and Molinari 1992] Y. Leroy and A. Molinari, "Stability of steady states in shear zones", *J. Mech. Phys. Solids* **40** (1992), 181–212.

[Lubliner 2008] J. Lubliner, *Plasticity theory*, Dover Publications, Mineola, NY, 2008.

[Needleman and Tvergaard 1992] A. Needleman and V. Tvergaard, "Analyses of plastic flow localization in metals", *Appl. Mech. Rev. (ASME)* **45**:3S (1992), 1394557.

[Perzyna 1966] P. Perzyna, "Fundamental problems in viscoplasticity", *Adv. Appl. Mech.* **9** (1966), 243–377.

[Regenauer-Lieb et al. 2013a] K. Regenauer-Lieb, M. Veveakis, T. Poulet, F. Wellmann, A. Karrech, J. Liu, J. Hauser, C. Schrank, O. Gaede, and M. Trefry, "Multiscale coupling and multiphysics approaches in earth sciences: applications", *J. Coupled Syst. Multiscale Dyn.* **1**:3 (2013), 281–323.

[Regenauer-Lieb et al. 2013b] K. Regenauer-Lieb, M. Veveakis, T. Poulet, F. Wellmann, A. Karrech, J. Liu, J. Hauser, C. Schrank, O. Gaede, and M. Trefry, "Multiscale coupling and multiphysics approaches in earth sciences: theory", *J. Coupled Syst. Multiscale Dyn.* **1**:1 (2013), 49–73.

[Rice 1977] J. R. Rice, "The localization of plastic deformation", pp. 207–220 in *14th International Congress on Theoretical and Applied Mechanics (ICTAM)* (Delft, Netherlands, 1976), edited by W. Koiter, North-Holland Publishing Company, Amsterdam, 1977.

[Rosakis et al. 2000] P. Rosakis, A. J. Rosakis, G. Ravichandran, and J. Hodowany, "A thermodynamic internal variable model for the partition of plastic work into heat and stored energy in metals", *J. Mech. Phys. Solids* **48**:3 (2000), 581–607.

[Rudnicki and Rice 1975] J. W. Rudnicki and J. R. Rice, "Conditions for the localization of deformation in pressure sensitive dilatant materials", *J. Mech. Phys. Solids* **23** (1975), 371–394.

[Taylor and Quinney 1934] G. Taylor and H. Quinney, "The latent energy remaining in a metal after cold working", *Proc. Royal Soc., Ser. A.* **143** (1934), 307–326.

[Vardoulakis 2002] I. Vardoulakis, "Steady shear and thermal run-away in clayey gouges", *Int. J. Solids Struct.* **39** (2002), 3831–3844.

[Veveakis et al. 2007] E. Veveakis, I. Vardoulakis, and G. D. Toro, "Thermoporomechanics of creeping landslides: the 1963 Vaiont slide, northern Italy", *J. Geophys. Res.* **112** (2007), F03026.

[Veveakis et al. 2010] E. Veveakis, S. Alevizos, and I. Vardoulakis, "Chemical reaction capping of thermal instabilities during shear of frictional faults", *J. Mech. Phys. Solids* **58**:9 (2010), 1175–1194.

[Veveakis et al. 2014] E. Veveakis, T. Poulet, and S. Alevizos, "Thermo-poro-mechanics of chemically active creeping faults, 2: transient considerations", *J. Geophys. Res.: Solid Earth* **119**:6 (2014), 4583–4605.

MARTIN K. PAESOLD: martin.paesold@gmail.com
School of Mathematics and Statistics, University of Western Australia, 35 Stirling Hwy, Crawley WA 6009, Australia
and
CSIRO Earth Science and Resource Engineering, 26 Dick Perry Avenue, Kensington, WA 6151, Australia

ANDREW P. BASSOM: andrew.bassom@utas.edu.au
School of Mathematics and Physics, University of Tasmania, Private Bag 37, Hobart TAS 7001, Australia
and
School of Mathematics and Statistics, University of Western Australia, 35 Stirling Hwy, Crawley, WA6009, Australia

KLAUS REGENAUER-LIEB: regenau@gmail.com
School of Petroleum Engineering, University of New South Wales, Tyree Energy Technologies Building, Anzac Parade, Kensington NSW 2052, Australia
e.veveakis@unsw.edu.au

MANOLIS VEVEAKIS: e.veveakis@unsw.edu.au

School of Petroleum Engineering, University of New South Wales, Tyree Energy Technologies Building, Anzac Parade, Kensington NSW 2052, Australia

and

School of Mathematics and Statistics, University of Western Australia, 35 Stirling Hwy, Crawley, WA6009, Australia

JOURNAL OF MECHANICS OF MATERIALS AND STRUCTURES

msp.org/jomms

Founded by Charles R. Steele and Marie-Louise Steele

Cover photo: Mando Gomez, www.mandolux.com